

Adversarial Purification and Fine-tuning for Robust UDC Image Restoration

Zhenbo Song, Zhenyuan Zhang, Kaihao Zhang, Zhaoxin Fan, Jianfeng Lu

Abstract—This study delves into the enhancement of Under-Display Camera (UDC) image restoration models, focusing on their robustness against adversarial attacks. Despite its innovative approach to seamless display integration, UDC technology faces unique image degradation challenges exacerbated by the susceptibility to adversarial perturbations. Our research initially conducts an in-depth robustness evaluation of deep-learning-based UDC image restoration models by employing several white-box and black-box attacking methods. This evaluation is pivotal in understanding the vulnerabilities of current UDC image restoration techniques. Following the assessment, we introduce a defense framework integrating adversarial purification with subsequent fine-tuning processes. First, our approach employs diffusion-based adversarial purification, effectively neutralizing adversarial perturbations. Then, we apply the fine-tuning methodologies to refine the image restoration models further, ensuring that the quality and fidelity of the restored images are maintained. The effectiveness of our proposed approach is validated through extensive experiments, showing marked improvements in resilience against typical adversarial attacks.

Index Terms—under-display-camera image restoration, deep learning, adversarial attacks, adversarial defense.

I. INTRODUCTION

THE advent of Under-Display Camera (UDC) technology marks a significant leap in the evolution of display technologies, particularly in the realm of smartphones and other personal electronic devices. UDCs offer an innovative solution to the long-standing challenge of balancing screen real estate with camera placement by seamlessly integrating cameras beneath display screens. This technology enables a full-screen experience without notches or punch-hole cameras, thus revolutionizing modern devices' design and aesthetic appeal. However, the integration of cameras under display panels introduces complex challenges in image restoration, primarily due to the interference of the display pixels with the camera's field of view. This results in inevitable image degradation issues like flare, blurring, color distortion, and contrast reduction [1].

Z. Song, Z. Zhang, and J. Lu are with the School of Computer Science and Engineering, Nanjing University of Science and Technology, Nanjing 210094, China. (Email: songzb@njust.edu.cn; zyZhang.bbetter@gmail.com; lujf@njust.edu.cn)

Kaihao Zhang is with the School of Computer Science and Technology, Harbin Institute of Technology, Shenzhen 518055, China. (Email: super.khzhang@gmail.com)

Zhaoxin Fan is with Renmin University of China, Beijing 100872, China (Email: fanzhaoxin@ruc.edu.cn)

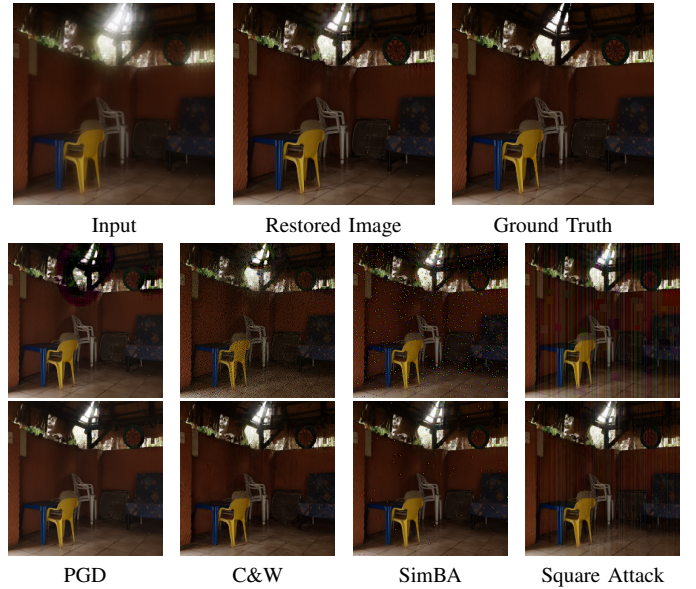


Fig. 1. The visualization results of our proposed defense strategy under different attacks. The second and third rows represent the results without any defense and with our proposed defense strategy, respectively. Best view by zooming in.

To address these challenges, evolving deep-learning-based image restoration methods [1]–[10] have been proposed in recent years for the recovery and enhancement of degraded UDC images. Most of these methods focus on accurately modeling the complex degradation process inherent in UDC systems and innovating new deep neural network architectures to enhance image restoration efficacy. The robustness of UDC image restoration models, particularly their resilience to subtle and often undetectable perturbations like adversarial attacks, has not been thoroughly explored. Given the prevalent application of UDC technology in smartphones, the vulnerability of UDC image restoration models to cyber threats, especially adversarial attacks, has emerged as a crucial area of concern. Such adversarial attacks can significantly aggravate existing image quality issues, posing a considerable risk to both the functionality and dependability of these devices. This underscores the need for research on UDC image restoration quality and the resilience and robustness of these deep models against adversarial attacks.

In this paper, we first comprehensively evaluate the adversarial robustness of deep-learning-based UDC image restoration models. To make a fair comparison of different mod-

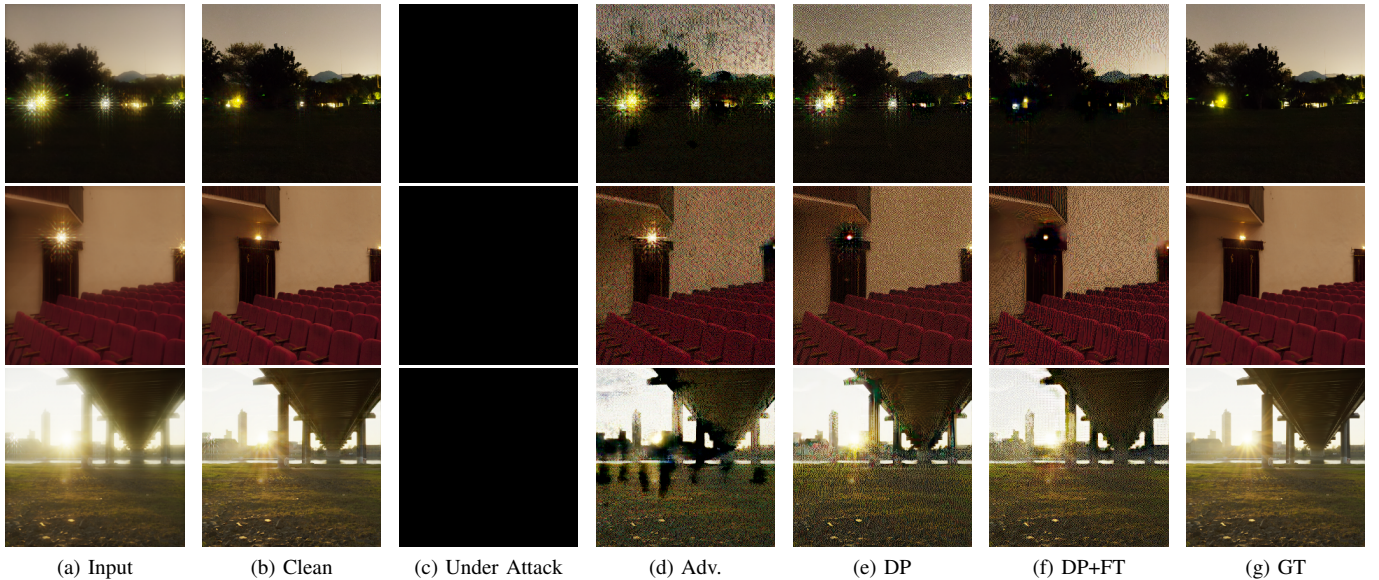


Fig. 2. Comparison of DISCNet with adversarial training and our proposed defense strategy under C&W attack on the synthetic dataset. Best view by zooming in.

approaches, ignoring those using particular degradation priors, *i.e.*, Point Spread Function (PSF) [11]. In the total of 7 networks are considered in our research, including architectures of CNN [12], [13], dynamic CNN [14], transformer [15]–[19], etc. We employ various sophisticated white-box and black-box attacking methods for a rigorous robustness evaluation process. White-box attacks have full knowledge and access to the models, making them ideal for thorough robustness testing. In contrast, black-box attacks have limited or no knowledge, aligning them more closely with real-world attack scenarios. Specifically, we use PGD [20] and C&W [21] for white-box attacks, and SimBA [22] and Square Attack [23] for black ones. This robustness evaluation is pivotal, as it reveals the weaknesses of the current UDC image restoration models and sets the stage for developing effective defense pipelines. We propose a novel defense framework that synergistically combines adversarial purification with fine-tuning processes to address adversarial vulnerabilities. Our approach leverages diffusion-based techniques [24]–[26], effectively negating the malicious perturbations introduced by adversarial attacks. Adversarial examples are purified before being fed into image restoration models. Subsequently, we employ fine-tuning methodologies to enhance the image restoration models further. This step is tailored to reinforce the models’ resilience against adversarial manipulations while improving their generalization to the original and purified images. Additionally, our fine-tuning strategy offers a more efficient pathway to achieving robust model performance than traditional adversarial training methods.

Overall, the primary contributions of this paper are three-fold: (1) We conduct an exhaustive evaluation of the adversarial robustness of current UDC image restoration models, which employ a range of white-box and black-box attacking methods, offering a comprehensive understanding of models’ vulnerabilities and resilience against various adversarial threats. (2) We propose a novel defense strategy which combines state-

of-the-art adversarial purification and fine-tuning techniques, providing an effective and efficient way to get a robust restoration model. (3) We carry out extensive experiments to investigate the robustness of the proposed defense method, which validates the achievement of more robust, reliable, and trustworthy UDC image restoration methods.

II. RELATED WORK

A. UDC Image Restoration

To the best of our knowledge, Zhou et-al. [1] were the first to address this new restoration challenge using deep learning, along with their 2020 ECCV challenge [27]. They created the Monitor-Camera Imaging System (MCIS) to enable the collection of real paired data in P-OLED and T-OLED. They also used a model-based data synthesis pipeline to produce point spread functions (PSF) and UDC data from only display patterns and camera measurements. They introduced an UNet-based [28] architecture for image denoising and deconvolution. To obtain a larger receptive field and save memory, Sundar et-al. [29] proposed a Deep Atrous Guided Filter network (DAGF), which utilizes restored low-resolution images to guide the restoration of high-resolution images. Feng et-al. [2] considered the significant impact of high dynamic range on data generation and PSF measurement. They used rigid UDC components instead of manually covering the camera with regular OLED. Their proposed DynamIc Skip Connection Network (DISCNet) fully utilized the conditional constraints of a long-tailed PSF to estimate the latent Clean image. Koh et-al. [3] proposed a dual-branch network that handles high-frequency and low-frequency components separately. They introduced affine transformation connections to eliminate noise and preserve the structure of the image. Liu et-al. [4] proposed a U-shape network to capture multiple spatial feature transformations. To balance the influence of pixels with different intensities in UDC images. Luo et-al. [5]

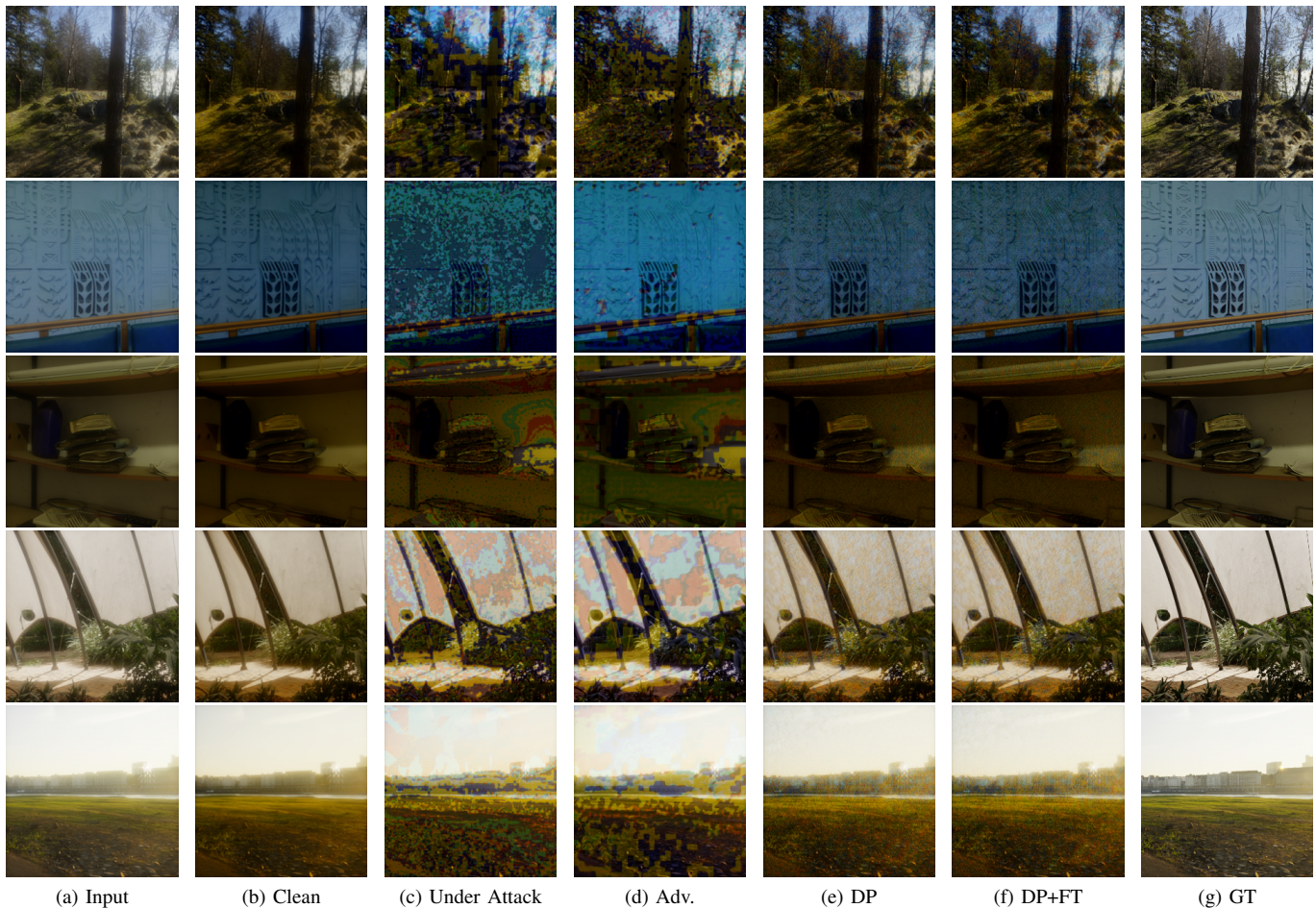


Fig. 3. Comparison of UFormer with adversarial training and our proposed defense strategy under C&W attack on the synthetic dataset. Best view by zooming in.

identified unique statistical characteristics of UDC and ground-truth images in HSV space. They proposed a cascaded curve estimation network to enhance UDC images by adaptively fitting the estimated images in H and S channels. Zhou et-al. [6] introduced GAN [30] to generate paired UDC images and proposed a transformer-based network to restore images. Song et-al. [7] considered the real physical scattering effects and utilized them to guide the image branch to restore an explicit scene.

B. General Adversarial Attacks and Defenses

Deep neural networks (DNNs) can misclassify images under the influence of imperceptible perturbations [31], [32]. Based on the adversary’s understanding of the victim model, existing adversarial attacks can be divided into white-box attacks (know all the information about the target model) and black-box attacks (can only observe the output results of the target model for input samples). The former mainly uses the gradient information of the network to generate adversarial samples, e.g., L-BFGS [33], FGSM [34], DeepFool [35], PGD [20], and C&W [21]. The latter mainly uses input-output model queries to generate adversarial samples, e.g., ZOO [36], SimBA [22], GeoDA [37], and Square Attack [23]. Attackers are not only

targeting computer vision tasks [38]–[40], but are also trying to harm other DNN-based tasks, such as natural language processing [41] and image generation [42].

To protect DNNs from adversarial attacks, adversarial defenses have evolved into two main branches: adversarial training and adversarial preprocessing. Adversarial training [31], [43], [44] involves training the network with adversarial samples, which enhances the robustness of itself. However, this technique can lead to the network becoming overly specialized in countering a specific type of attack, thereby diminishing its performance on clean images [45], [46]. Adversarial purification [47], [48] is one of the typical preprocessing methods, aiming to transform adversarial samples into clean samples. Generative methods such as GAN [30], VAE [49], and Diffusion [24] are widely applied, for example, Defense-GAN [50], A-VAE [51], and DiffPure [26].

C. Adversarially Robust Image Restoration

Recent research has explored the topic of adversarial attacks in low-level image restoration tasks, such as derain [52], super-resolution [53]–[55], dehaze [40], deblur [38], and reflection removal [56]. Yu et-al. [52] systematically investigated the impact of critical modules on the robustness of rain removal

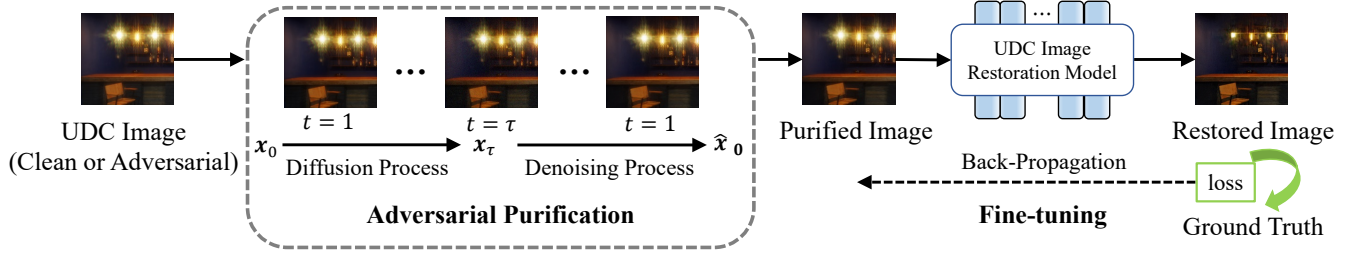


Fig. 4. The overall pipeline of our proposed defense strategy for under-display camera image restoration.

models against adversarial attacks. They evaluated the models' ability to withstand adversarial attacks from both human and machine vision perspectives and their impact on downstream tasks. Yue et-al. [55] focused on eliminating adversarial noise in the frequency domain of super-resolution models. Gui et-al. [40] proposed five adapted attack methods for the dehaze problem. Song et-al. [56] conducted a comprehensive study on the robustness of reflection removal models against adversarial attacks, considering different attack methods, attack levels, and attack regions. They proposed a robust reflection removal model integrating cross-scale attention modules, multi-scale fusion modules, and an adversarial image discriminator.

However, there is no research on robust networks against adversarial attacks in UDC image restoration. Evaluation of adversarial attacks and appropriate attack methods are also necessary.

In this work, we mainly explore the impact of adversarial attacks on the robustness of image restoration, which is necessary. We have chosen white-box and black-box attacks to comprehensively examine the robustness of UDC recovery methods under adversarial attacks. The former uses PGD attacks and C&W attacks, while the latter uses SimBA and Square Attack. Notably, setting different attack targets and attack difficulties in the PGD attack can provide a comprehensive measure of adversarial robustness.

III. ADVERSARIAL ATTACKS ON UDC IR

Similar to adversarial attacks on other image restoration tasks [38], [56], the critical element in UDC adversarial attacks is the creation of visually imperceptible perturbations on the input images. The perturbations must be specifically tailored to the restoration models, ensuring they do not substantially degrade the visual quality. This aspect is vital, as the primary objective of adversarial attacks is to subtly influence the outcomes of the restoration process through the introduction of noise rather than to overtly reduce the quality of UDC images, which would merely increase the complexity of the restoration task. We incorporate sample-specific noise maps into the input UDC images pixel-wise while limiting the range of perturbations to ensure they are visually indistinguishable.

Mathematically, given \mathbf{x} as a UDC image, the adversarial attack generates a pixel-wise noise map δ according to the image restoration model $f(\cdot; \psi)$, where ψ represents the parameters of the model. The goal is to create an adversarial example \mathbf{x}_{adv} from an original image \mathbf{x} , such that the perturbation δ

is small but effective enough to fool the model. This can be formulated as:

$$\mathbf{x}_{adv} = \mathbf{x} + \delta, \quad \text{where} \quad \|\delta\|_{\ell} < \epsilon \quad (1)$$

Here ϵ is a small constant that controls the magnitude of the perturbation. Given the original restored image \mathbf{y} without adversarial attacks, where $\mathbf{y} = f(\mathbf{x}; \psi)$, the adversarial example is crafted to maximize the loss function $J(f(\mathbf{x}_{adv}; \psi), \mathbf{y})$:

$$\delta = \arg \max_{\|\delta\|_{\ell} < \epsilon} J(f(\mathbf{x}_{adv}; \psi), \mathbf{y}) \quad (2)$$

The loss function $J(\cdot, \cdot)$ quantifies the disparity between restored images with and without adversarial attacks. Accordingly, there are two types of loss functions utilized in adversarial attacks [56]. The first type centers around pixel-wise image discrepancy, commonly measured by metrics like Mean Squared Error (MSE). Conversely, the second objective prioritizes the high-level perceptual similarity of output images, such as LPIPS [57].

A. White-Box Attacks

For white-box attacks, the attackers have full access to the UDC image restoration model. This is to say that, in Equ. 2, the architecture of f and the parameters ψ are known to the attackers. Thus, we choose two typical adversarial attackers, the PGD and the C&W.

PGD is an iterative method commonly used for adversarial training and robustness testing of neural networks [38], [56]. It works by making small, calculated adjustments to the input UDC image \mathbf{x} in the direction that increases the loss function $J(f(\mathbf{x}_{adv}; \psi), \mathbf{y})$, while ensuring that $\|\mathbf{x}_{adv} - \mathbf{x}\|_{\ell} < \epsilon$. Here ℓ indicates the chosen norm, typically $L-\infty$, that bounds the adversarial perturbations.

Compared to PGD, C&W focuses on minimizing the perturbations δ , resulting in more subtle and harder-to-detect adversarial examples. This method is mainly known for its precision and effectiveness in crafting less perceptible perturbations. Especially in its $L2$ variant, it aims at creating the smallest possible perturbations.

B. Black-Box Attacks

For black-box attacks, the attackers can only observe the outputs of UDC image restoration models. In other words, there is only information about the clean outputs \mathbf{y} , as well

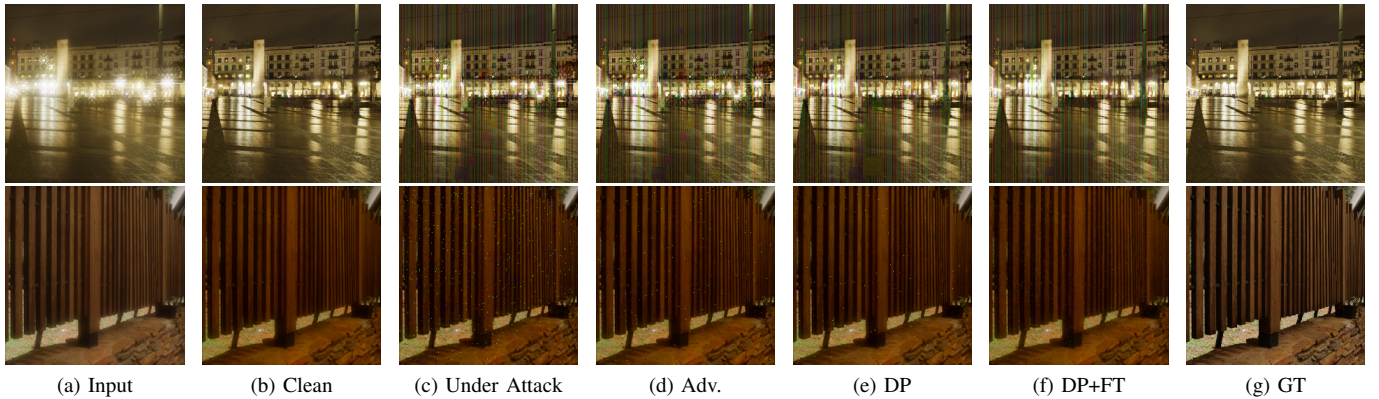


Fig. 5. Comparison of adversarial training and our proposed defense strategy regarding different black attack methods on the synthetic dataset. The first row represents the performance of DISCNet [2] under Square attack. The second row represents the performance of UFormer [58] under SimBA, respectively. Best view by zooming in.

as the adversarial outputs $f(\mathbf{x}_{adv}; \psi)$. Hence, δ is generated using a substitute restoration model or trial-and-error methods. This paper applies the SimBA and Square attack approaches to perform black-box attacks.

SimBA operates by randomly perturbing individual pixels or small groups of pixels in the UDC image and observing the changes in the model’s output. SimBA does not require gradient information or internal knowledge of the restoration model, making it broadly applicable and straightforward to implement.

Square Attack is another black-box method that generates adversarial examples by modifying a random contiguous square area in the UDC image. This approach is more query-efficient than SimBA, often achieving higher success rates with fewer queries. However, this might result in more visually noticeable perturbations compared to pixel-wise methods like SimBA.

IV. ADVERSARIAL PURIFICATION AND FINE-TUNING

Existing image restoration models accomplish the adversarial robustness by predominantly analyzing the contributions of network modules to robustness. With a combination of robust modules, novel network architectures are designed to detect or remove adversarial perturbations. Moreover, adversarial training techniques are incorporated to bolster the model’s resilience further. However, adversarial training can be time-consuming and inefficient. Besides, training for robustness often necessitates a trade-off between performance on clean (unperturbed) images and adversarial (perturbed) images, which can adversely impact the restoration quality for clean inputs [59].

Instead of constructing new neural network models, we propose to purify adversarial perturbations. Specifically, we utilize a preprocessing module to remove adversarial noise from input UDC images. It could be compatible with a variety of restoration networks or modules. Ideally, any pre-trained UDC image restoration models can be seamlessly integrated after the purification. However, the purification could also denoise the degradation of UDC images to a certain, causing domain discrepancy to the original UDC images. To accelerate

the adaptation of the restoration model to the purified outputs, we create a specialized fine-tuning strategy without the need for adversarial training data. The fine-tuning facilitates more effective and rapid model adjustment to the purified data. The whole defense pipeline is illustrated in 4.

A. Adversarial Purification

Adversarial purification aims to neutralize the impact of adversarial perturbations in the input UDC images. Let $\hat{\mathbf{x}}_0$ be the purified image, and model the purification process as $p_\phi(\hat{\mathbf{x}}_0|\mathbf{x})$. Here, ϕ denotes the parameters of the purification model. Inspired by [26], [60], \mathbf{x} is first corrupted to a noisy status through a diffusion process, typically using DDPM [24]. For simplicity, we denote the \mathbf{x} as \mathbf{x}_0 at timestep 0, and the forward process is formulated as:

$$q(\mathbf{x}_t|\mathbf{x}_{t-1}) = \mathcal{N}(\mathbf{x}_t; \sqrt{1 - \beta_t}\mathbf{x}_{t-1}, \beta_t\mathbf{I}) \quad (3)$$

where \mathbf{x}_t is the data at timestep t , β_t is the pre-defined noise level, and \mathcal{N} denotes the normal distribution. Based on the Markov Chain, for a specific timestep τ , the noisy distribution can be calculated as:

$$\begin{aligned} q(\mathbf{x}_\tau|\mathbf{x}_0) &= \mathcal{N}(\mathbf{x}_\tau; \sqrt{\bar{\alpha}_\tau}\mathbf{x}_0, \sqrt{1 - \bar{\alpha}_\tau}\mathbf{I}) \\ &= \sqrt{\bar{\alpha}_\tau}\mathbf{x}_0 + \sqrt{1 - \bar{\alpha}_\tau}\boldsymbol{\epsilon} \end{aligned} \quad (4)$$

Here, $\bar{\alpha}_\tau$ represents the cumulative multiplication from $t = 1$ to $t = \tau$, and $\boldsymbol{\epsilon}$ follows the standard normal distribution $\mathcal{N}(\mathbf{0}, \mathbf{I})$. As τ increasing, the distribution of \mathbf{x}_τ eventually satisfies $\mathcal{N}(\mathbf{0}, \mathbf{I})$. Intuitively, the adversarial image \mathbf{x}_{adv} could also be diffused as $\mathbf{x}_{adv}^\tau \sim \mathcal{N}(\mathbf{0}, \mathbf{I})$ when the timestep τ is large enough. Thus, the clean and adversarial image distributions get closer over the forward diffusion process [26]. This indicates that the adversarial perturbations could be gradually purified by adding specific noises. Since adversarial perturbations are typically small, there is no need for many timesteps to disperse the input UDC image. Empirically, around 100 steps are sufficient to attain close enough noisy images, whether inputting the adversarial image or the corresponding clean one.

Subsequently, the reverse process in DDPM is used to reconstruct the purified image $\hat{\mathbf{x}}_0$ from the noisy image. It can be described as a reverse Markov Chain that iteratively

denoises the data at each timestep. The reverse process for a specific timestep t is given by:

$$p_{\theta}(\mathbf{x}_{t-1}|\mathbf{x}_t) = \mathcal{N}(\mathbf{x}_{t-1}; \mu_{\theta}(\mathbf{x}_t, t), \Sigma_{\theta}(\mathbf{x}_t, t)) \quad (5)$$

Here, $\mu_{\theta}(\mathbf{x}_t, t)$ and $\Sigma_{\theta}(\mathbf{x}_t, t)$ are the mean and covariance of the Gaussian distribution at timestep t , which are parameterized by the neural network with parameters θ . Starting from \mathbf{x}_{τ} , the reverse process iteratively refines \mathbf{x}_t to approximate $\hat{\mathbf{x}}_0$, and finally accomplishes the purification pipeline.

Since the DDPM is typically trained with high-quality images, the purified image may not maintain the UDC features. For some image restoration tasks, e.g., face restoration [60], the adversarial purification could even become a degradation remover. This forms new challenges for pre-trained UDC image restoration networks because these networks are trained specially for such degradation patterns. They have less generalization to recover the purified UDC image. Hence, the fine-tuning strategy is further proposed and introduced as follows.

B. Model Fine-tuning

To fine-tune the UDC image restoration model, we generate purified images with different timesteps for increasing sample diversity. As mentioned above, purified images should share the same distribution for clean and adversarial UDC inputs. Hence, adversarial training is not necessary for the model fine-tuning. Moreover, during the fine-tuning phase, the parameters of the purification network are held constant, ensuring stability and consistency in the purification process.

For symbolic expression, let $g(\cdot, t; \phi)$ denote the purification model. The purified UDC image \mathbf{x}_{pur} is obtained by $\mathbf{x}_{pur} = g(\mathbf{x}, t^*; \phi)$. Unlike the real purification phase, there is no need to strictly large enough timestep t^* . Limited diffusion and denoising steps could also help improve the diversity of UDC samples. Through this method, training efficiency can be greatly raised.

Regarding the loss function for fine-tuning, we employ supervised losses to minimize the discrepancy between the new prediction and the ground truth. Let $\mathcal{L}(\cdot, \cdot)$ represent the in total loss function. The fine-tuning can be formulated as:

$$\psi^* = \arg \min_{\psi} \mathcal{L}(f(\mathbf{x}_{pur}; \psi), \mathbf{x}_{gt}) \quad (6)$$

where \mathbf{x}_{gt} the ground truth image without UDC effects. The loss function is a linear combination of typical image reconstruction loss terms, such as Euclidean loss, GAN loss, perceptual loss, etc. We adaptively utilize loss terms consistent with training original UDC image restoration models.

Our approach mitigates the immediate effects of adversarial attacks through these two stages and reinforces the model's long-term resilience to such perturbations.

V. EXPERIMENTS

A. Implementation Details

Dataset. For the dataset, we synthesize the dataset using nine existing ZTE Axon 20 phone PSFs and one real-scene PSF [61], following [2], [7]. We generate a total of 21,060 training image pairs and 3,600 testing image pairs from the 2,016

training images and 360 testing images, which are collected from the HDRI Haven dataset [62].

UDC IR methods. We select six state-of-the-art UDCIR methods for comparison, including DAGF [29], DISCNet [2], UDCUNet [4], BNUDC [3], SRUDC [7], and DWFormer [6]. We also include a general image restoration method called UFormer [58] for a comprehensive evaluation. All the methods are re-trained on the training dataset with the same parameters set to ensure a fair comparison. We adopt PSNR [63] and SSIM [64] as the evaluation metrics.

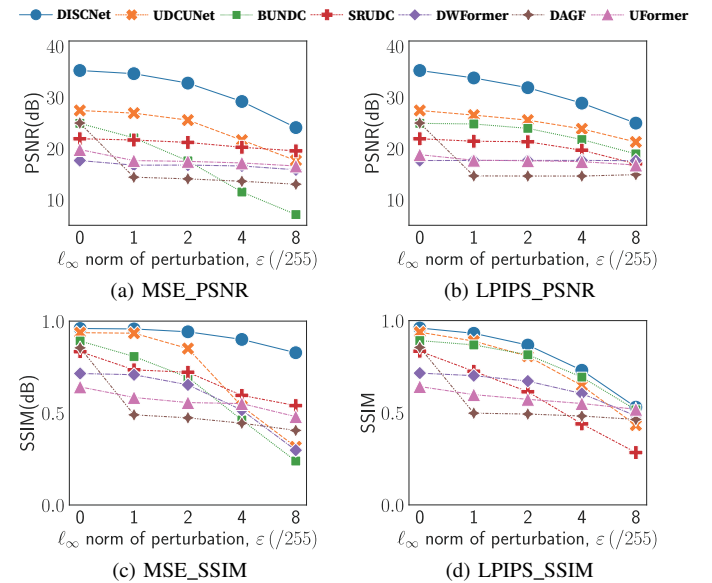


Fig. 6. Comparison of the PSNR and SSIM values with respect to perturbation levels ϵ . ‘MSE_PSNR’ represents the PSNR values, attacking the MSE objective and others. Best view by zooming in.

B. Robustness Evaluation on Attack Methods Comparison

From the aspect of PSNR. Table I compares the PSNR performance of various deep UDCIR methods under different attack methods. All methods experience a significant decrease in performance after being subjected to adversarial attacks. DISCNet demonstrates the best performance in clean images with the PSNR of 35.237. UDCUNet and DAGF also perform well, with the PSNR of 27.427 and 24.911, respectively. DWFormer and UFormer exhibit relatively lower performance. This can be attributed to the fact that DWFormer was trained on the TOLED&POLED dataset [1] and has a more significant number of parameters. The limited size of the training set and the larger model size prevent UFormer from fully leveraging its performance capabilities.

To comprehensively analyze the impact of different attacks on the robustness of various methods, we present our findings from two perspectives:

- 1) **Single attack method on different restoration methods.** In terms of PGD, this type of attack generally decreased the performance of all models. The performance of DAGF witnessed the most substantial decline, dropping from 24.972 to 13.772. BNUDC experienced the second most prominent decrease, going from

TABLE I

COMPARISON OF DIFFERENT ATTACK METHODS ON THE SYNTHETIC DATASET IN TERMS OF **PSNR**. SQUAREA DENOTES THE SQUARE ATTACK [23]. **BOLD** AND UNDERLINE INDICATE THE MOST SEVERE AND SECOND MOST SEVERE DEGRADATION, RESPECTIVELY.

Method	DISCNet [2]	UDCUNet [4]	BNUDC [3]	SRUDC [7]	DWFormer [6]	DAGF [29]	UFormer [58]
Clean	35.237	27.427	24.911	21.904	17.651	24.972	19.795
Attack	PGD	30.166	22.936	<u>14.565</u>	20.656	16.484	13.772
	C&W	15.158	14.279	<u>7.501</u>	5.985	13.760	11.796
	SimBA	20.578	19.766	24.059	20.747	15.786	<u>14.794</u>
	SquareA	25.018	21.557	22.986	20.300	5.985	<u>13.454</u>

TABLE II

COMPARISON OF DIFFERENT ATTACK OBJECTIVES IN PGD ON THE SYNTHETIC DATASET IN TERMS OF **PSNR**. CLEAR, MSE, AND LPIPS DENOTE CORRESPONDING CLEAR IMAGES, MSE, AND LPIPS OBJECTIVES. **BOLD** AND UNDERLINE INDICATE THE MOST SEVERE AND SECOND MOST SEVERE DEGRADATION, RESPECTIVELY.

Method	Clean	MSE	LPIPS
DISCNet [2]	35.237	30.166	<u>29.870</u>
UDCUNet [4]	27.427	22.936	24.293
BNUDC [3]	24.911	<u>14.565</u>	22.356
SRUDC [7]	21.904	20.656	19.853
DWFormer [6]	17.651	16.484	17.658
DAGF [29]	24.972	13.772	14.695
UFormer [58]	18.795	17.222	17.383

24.911 to 14.565. However, DISCNet and UDCUNet showed better restoration performance, indicating their robustness in handling such attacks. In terms of C&W, most models saw a significant decline in performance, particularly DISCNet and UDCUNet. UFormer, on the other hand, demonstrated significant robustness. In terms of SimBA, the impact of attacking UDCIR methods was relatively minor, with no significant vulnerabilities exposed. DISCNet and BNUDC exhibited a slight advantage in maintaining stable performance. In terms of square attack, the results showed notable differences in impact across different models. UFormer and DISCNet were more effective in dealing with such attacks, while DWFormer was particularly sensitive to square attack, exhibiting a considerable decline in performance.

- 2) **Single restoration method against different attack methods.** DISCNet exhibits overall strong performance, excelling in handling clean images and maintaining high effectiveness under various attack types. However, it shows notable sensitivity to C&W attack, suggesting a potential weakness in its resilience against this specific type of adversarial attack. UDCUNet demonstrates robustness across attack scenarios, showcasing balanced

performance under various adversarial conditions. Despite this, the model reveals a sensitivity to C&W attack, with a noticeable decline in performance when subjected to this particular form of attack. BNUDC stands out for its excellent performance under SimBA attacks, showcasing superior capabilities in the face of this specific adversarial technique. However, its performance experiences significant drops under other attack types, mainly exhibiting vulnerability to C&W attack, indicating the need for additional optimization or protective measures. DWFormer reveals vulnerability to square attack, displaying the weakest performance under this specific adversarial condition. Its general performance is average across other attack types and clean image processing, lacking standout achievements compared to its counterparts. UFormer demonstrates remarkable resilience under C&W attacks, highlighting its strength in maintaining robustness against this particular form of adversarial assault. The model exhibits balanced performance, showing competency in handling clean images and various attack types without specific weaknesses.

In summary, the results of the robustness evaluation reveal that the current UDCIR methods are vulnerable to adversarial attacks. The performance of these models is significantly degraded under various adversarial conditions, particularly when subjected to C&W attack. DISCNet demonstrates superior performance when dealing with clean images, boasting the highest Clean accuracy. However, in terms of robustness, UFormer exhibits relatively better performance across various attack methods, including PGD, C&W, SimBA, and SquareA, showcasing a more comprehensive resilience.

From the aspect of SSIM. Table III compares the SSIM performance of these methods under different attack methods. Overall, DISCNet stands out as the most effective method. It leads with 0.960 in processing clean images and maintains the top position with an average performance SSIM of 0.551 under four different attack methods. This indicates that DISCNet is best dealing with unattacked clean images and demonstrates the strongest resilience and best overall performance under various attacks. To obtain a more detailed and comprehensive understanding of the robustness of different UDCIR methods against various attack methods, we analyze this table from two perspectives:

- 1) **Single attack method on different restoration methods.** Regarding specific attack methods, different meth-

TABLE III

COMPARISON OF DIFFERENT ATTACK METHODS ON THE SYNTHETIC DATASET IN TERMS OF **SSIM**. SQUAREA DENOTES THE SQUARE ATTACK [23]. **BOLD** AND UNDERLINE INDICATE THE MOST SEVERE AND SECOND MOST SEVERE DEGRADATION, RESPECTIVELY.

Method	DISCNet [2]	UDCUNet [4]	BNUDC [3]	SRUDC [7]	DWFormer [6]	DAGF [29]	UFormer [58]
Clean	0.960	0.937	0.8917	0.834	0.715	0.855	0.642
Attack	PGD	0.907	0.66	0.551	0.648	0.544	0.543
	C&W	0.207	0.237	0.185	0.019	0.157	0.441
	SimBA	0.529	0.548	0.805	0.715	0.687	0.581
	SquareA	0.559	0.466	0.652	0.469	0.019	0.546

ods have their respective strengths. For instance, while DISCNet shows the best resistance against PGD and Square attack, BNUDC and SRUDC perform better under SimBA. UFormer, on the other hand, indicates relatively better performance against the C&W attack.

- 2) **Single restoration method against different attack methods.** In terms of PGD attack, DISCNet demonstrates superior resilience, achieving the highest SSIM of 0.907. This indicates its effectiveness in countering this type of attack. Conversely, UDCUNet and UFormer show more vulnerability with SSIM of 0.660 and 0.543, respectively, suggesting a greater sensitivity to PGD attacks. In terms of the C&W attack, a notable shift in performance is observed. UFormer emerges as the most resistant, with the SSIM of 0.441, indicating its strength against this sophisticated attack method. Conversely, SRUDC shows significant vulnerability, scoring only 0.019, highlighting its weak defense against CW attacks. In terms of SimBA, BNUDC, and SRUDC exhibit commendable resilience, scoring 0.805 and 0.715, respectively. These scores reflect their robustness in scenarios where the attacker’s strategy is not fully known, a key strength for black-box attack scenarios. In contrast, DISCNet and DAGF show comparatively weaker performance under SimBA attacks. In terms of Square Attack, DISCNet again stands out, with the SSIM of 0.559, which underscores its effectiveness in repelling this efficient and effective attack. Conversely, DWFormer demonstrates a significant lack of resistance with a score of 0.019, pointing to its vulnerability to Square Attack.

In conclusion, the robustness evaluation indicates that current UDCIR methods are susceptible to adversarial attacks. DISCNet [2] demonstrates excellent performance when handling clean images. However, in terms of robustness, UFormer [58] exhibits relatively better performance across various attack methods.

C. Robustness Evaluation on Attack Objectives Comparison

From the aspect of PSNR. Table II shows the PSNR performance of various deep UDCIR methods under different attack objectives in PGD attack. Analyzing the data reveals a trend indicating that the MSE objective tends to induce more pronounced degradation than the LPIPS objective. For DISCNet, SRUDC, DWFormer, DAGF, and UFormer, there is a marginal

TABLE IV

COMPARISON OF ADVERSARIAL TRAINING AND OUR PROPOSED DEFENSE STRATEGY IN TERMS OF DIFFERENT ATTACK OBJECTIVES IN PGD ON THE SYNTHETIC DATASET IN TERMS OF **PSNR**. DP REFERS TO THE UTILIZATION OF DIFFPURE, WHEREAS FT INDICATES THE IMPLEMENTATION OF FINE-TUNING.

Method	Clean	MSE	LPIPS
DISCNet Adv. [2]	34.082	30.181	29.379
UFormer Adv. [58]	18.819	18.187	18.205
DISCNet [2] + DP	32.773	31.253	31.286
UFormer [58] + DP	18.950	18.391	18.766
DISCNet [2] + DP + FT	34.942	32.167	32.493
UFormer [58] + DP + FT	19.938	19.312	19.710

difference in performance following both types of attacks, with variations of approximately 1.000. However, BNUDC exhibits a notable contrast, experiencing a significant drop in PSNR from 24.911 to 14.565 under the MSE objective, while the LPIPS objective results in a PSNR decrease to 22.356 from 24.911. Although the MSE objective performs comparably to the LPIPS objective in more challenging restoration methods, it outperforms the latter in specific instances.

From the aspect of SSIM. Table V compares the SSIM performance of different attack objectives in PGD. It can be observed that the MSE objective yields more effective results compared to the LPIPS objective for most restoration methods. DISCNet and BNUDC exhibit poorer robustness when facing the LPIPS objective, primarily attributed to their utilization of VGG-based [65] visual loss methods. Other methods are more susceptible to the MSE objective.

D. Robustness Evaluation on Attack Levels Comparison

Fig. 6 illustrates the variations of PSNR and SSIM under different perturbation levels. As the perturbation level increases, the output quality of all methods noticeably deteriorates. As shown in Fig. 6a, BNUDC exhibits the highest sensitivity to attack difficulty, with its restoration performance declining the most with increasing perturbation. DISCNet and UDCUNet also experience significant decreases. On the

TABLE V

COMPARISON OF DIFFERENT ATTACK OBJECTIVES IN PGD ON THE SYNTHETIC DATASET IN TERMS OF **SSIM**. **CLEAR**, **MSE**, AND **LPIPS** DENOTE CORRESPONDING CLEAR IMAGES, **MSE**, AND **LPIPS** OBJECTIVES. **BOLD** AND **UNDERLINE** INDICATE THE MOST SEVERE AND SECOND MOST SEVERE DEGRADATION, RESPECTIVELY.

Method	Clean	MSE	LPIPS
DISCNet [2]	0.960	0.907	0.765
UDCUNet [4]	0.937	0.660	0.694
BNUDC [3]	0.892	0.551	0.723
SRUDC [7]	0.834	0.648	0.516
DWFormer [6]	0.715	0.544	0.615
DAGF [29]	0.855	0.454	0.484
UFormer [58]	0.642	0.543	0.560

other hand, DWFormer, DAGF, and UFormer exhibit sudden drops after being subjected to minimal difficulty attacks, especially DAGF, but subsequently become less sensitive to noise. SRUDC maintains robustness throughout. In Fig. 6b, most methods show relatively moderate decreases. Only DAGF experiences a sudden drop when facing attacks but remains insensitive afterward.

In terms of the SSIM, as shown in Fig. 6c and 6d, BNUDC and SRUDC demonstrate noticeable downward trends, indicating that the attack methods have a more significant impact on the structural aspects of the recovered images. DISCNet performs better under the MSE attack than the LPIPS attack objective. The decline in UDCUNet is no longer gradual, as it experiences a significant drop when perturbation $\epsilon = 4$. Additionally, DWFormer and UFormer exhibit significant performance fluctuations after the attack, suggesting that their models are more sensitive to noise in restoring image structures.

E. Defense Strategy Results

As mentioned in Sec. V-A, among all the methods evaluated, DISCNet [2] demonstrates superior restoration performance, while UFormer [58] exhibits exceptional robustness. To ensure a fair comparison, we conducted adversarial training on both methods. We extensively compared the results of adversarial training with our proposed defense strategy.

PGD Objective Comparison. Table IV presents the PSNR performance of adversarial training and our proposed defense strategy with PGD attack. After undergoing **adversarial training**, DISCNet exhibits improved robustness against PGD attack, but its restoration performance on clean images slightly decreases from 35.237 to 34.082. UFormer, on the other hand, shows a significant improvement in robustness after adversarial training, while its performance on clean images remains relatively unchanged. When only implementing the **DiffPure (DP)**

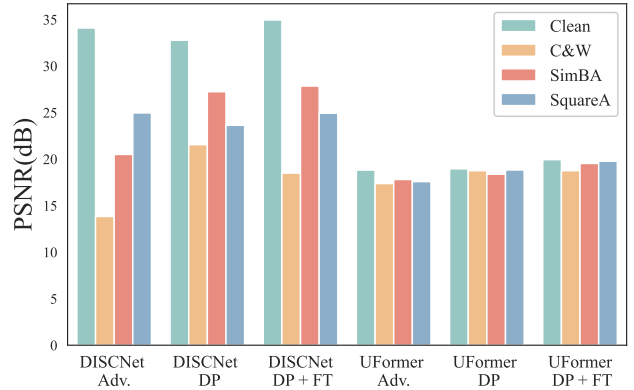


Fig. 7. Comparison of adversarial training and our proposed defense strategy in terms of different attack methods on the synthetic dataset. DP refers to the utilization of DiffPure, whereas FT indicates the implementation of Fine-tuning.

strategy, DISCNet experiences a more noticeable decline in performance on clean images, while UFormer shows a slight improvement. This suggests that DISCNet is more sensitive to noise. However, when implementing **our proposed defense strategy**, UFormer demonstrates a significant improvement in performance on clean images compared to the original model, increasing from 18.795 to 19.312. DISCNet's performance remains similar to the original model on clean images, but its robustness significantly improves when under attack.

Table IV compares the SSIM performance of adversarial training and our proposed defense strategy in terms of different attack objectives in PGD. Upon the application of **adversarial training**, DISCNet manifests a nominal decrement in its efficacy on clean images, evidenced by a reduction in metric from 0.960 to 0.956. Concurrently, its robustness is incremental enhancement against MSE attack and LPIPS attack adversarial vectors, with performance indices improving to 0.908 and 0.763, respectively. Integrating the **DiffPure (DP) strategy** into DISCNet precipitates a substantial diminution in its performance with clean images, descending from a score of 0.960 to 0.872. Nonetheless, this approach markedly bolsters its resilience against MSE attack and LPIPS attack, with performance indices ascending to 0.856 in both cases. The amalgamation of **our proposed defense strategy** in DISCNet results in a slight regression on clean images, decreasing from 0.960 to 0.945. However, this strategy culminates in a substantial elevation in its adversarial defense indices against MSE attack and LPIPS attack, soaring to 0.928 and 0.929, respectively.

In summary, our proposed defense strategy effectively elevates their robustness against adversarial attacks while concurrently preserving or augmenting their innate capabilities on clean images. It offers a balanced and productive solution to the clean challenge of bolstering adversarial robustness without eroding performance on clean images.

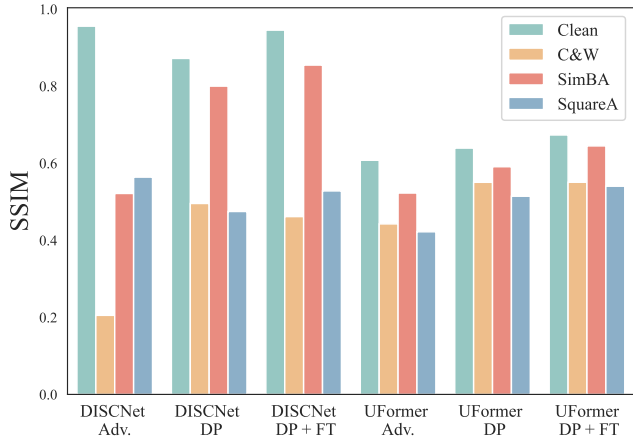


Fig. 8. Comparison of SSIM for adversarial training and our proposed defense strategy in terms of different attack methods on the synthetic dataset. DP refers to the utilization of DiffPure, whereas FT indicates the implementation of Fine-tuning.

F. Other Attack Methods Comparison

In Fig. 7, we also present the PSNR performance of adversarial training and our proposed defense strategy when facing C&W, square attack, and SimBA. Even after adversarial training, we can observe that DISCNet and UFormer still exhibit significant degradation under C&W attack, but they demonstrate better robustness against square attack. When only implementing the DP strategy, DISCNet and UFormer show noticeable improvements in robustness against C&W attacks, indicating that the DP strategy is more effective in defending against C&W attacks. However, in this case, we can see that both methods experience a decline in performance on clean images, attributed to DP’s introduction of additional small-scale noise. When implementing our proposed defense strategy, DISCNet, and UFormer also show significant improvements in robustness against these three attacks. At the same time, their performance on clean images is even better and surpasses that of the original model.

Fig. 8 compares the SSIM performance of adversarial training and our proposed defense strategy in terms of other attack methods, e.g., C&W, SimBA, and square attack. DISCNet and UFormer exhibit significant degradation under the C&W attack, while both perform well in defending against SimBA. When only DP is implemented, DISCNet and UFormer show improved robustness against C&W and SimBA. After implementing our proposed defense strategy, DISCNet demonstrates the best robustness against SimBA and square attack, comparable to adversarial training under C&W attack, while maintaining excellent performance on clean images. UFormer showcases superior robustness across all attack methods while delivering outstanding performance on clean images.

G. Visual Comparison.

Comparison of DISCNet under C&W attack with different defense strategies. In Fig. 2, we present visual results of DISCNet with adversarial training and our proposed defense

strategy under C&W attack. DISCNet fails to perform image restoration after being attacked, resulting in a completely black image. When adversarial training is applied, the attacked images exhibit black color patches and noticeable glare. Light diffusion is a significant phenomenon in the second row of images. When only DP is applied, there is a noticeable improvement in glare and irregular color patches in the images. However, some irregular color patches are still present, especially in the second row of images. When our proposed defense strategy is implemented, the diffusion around the light source in the images of the second row is significantly reduced. Similarly, no irregular color patches are observed in the images of the third row.

Comparison of UFormer under C&W attack with different defense strategies. In Fig. 3, we present additional visual results of the UFormer under the C&W attack. From the third column, it can be observed that UFormer exhibits numerous irregular patches when subjected to adversarial attacks, making it challenging to recover the original image. When adversarial training is applied, there is a slight improvement in the appearance of irregular patches in the visual results compared to the previous case. However, in the fifth and sixth columns, significant improvements in the appearance of irregular patches are observed when using both our proposed defense strategy and the only DP. Compared to the results obtained from clean images, our proposed defense strategy can preserve the overall structure of the original image and maintain good robustness.

Comparison of DISCNet and UFormer under black attack with different defense strategies. Fig. 5 visually compares adversarial training and our proposed defense strategy when facing square attack and SimBA. Based on the first-row images, it can be seen that DISCNet exhibits noticeable large and small blocks of colors when subjected to square attacks. When our proposed method is implemented, these blocks of colors are significantly reduced, and the glare issue is well resolved. Moreover, in the second-row images, it can be seen that UFormer performs better when subjected to Simba attacks with the application of our method.

VI. CONCLUSION

In this research, we thoroughly investigated the robustness of Under-Display Camera (UDC) image restoration models against adversarial attacks. Our comprehensive evaluation, utilizing white-box and black-box methods, identified significant vulnerabilities in current deep-learning-based UDC image restoration models. We introduced a novel defense framework that synergizes adversarial purification with fine-tuning processes to address these challenges. The diffusion-based purification stage proved highly effective in mitigating adversarial perturbations. Subsequent fine-tuning further reinforced the models’ resilience, enhancing the quality and integrity of the restored images. Extensive experiments demonstrated considerable improvements in robustness against diverse adversarial attack types. This study contributes significantly to UDC image processing technology and offers insights for developing robust deep learning models for image restoration amidst evolving adversarial threats.

REFERENCES

- [1] Y. Zhou, D. Ren, N. Emerton, S. Lim, and T. Large, "Image Restoration for Under-Display Camera," Mar. 2021.
- [2] R. Feng, C. Li, H. Chen, S. Li, C. C. Loy, and J. Gu, "Removing Diffraction Image Artifacts in Under-Display Camera via Dynamic Skip Connection Network," Apr. 2021.
- [3] J. Koh, J. Lee, and S. Yoon, "BNUDC: A Two-Branch Deep Neural Network for Restoring Images from Under-Display Cameras," in *2022 IEEE/CVF Conference on Computer Vision and Pattern Recognition (CVPR)*. New Orleans, LA, USA: IEEE, Jun. 2022, pp. 1940–1949.
- [4] X. Liu, J. Hu, X. Chen, and C. Dong, "UDC-UNet: Under-Display Camera Image Restoration via U-Shape Dynamic Network," Sep. 2022.
- [5] J. Luo, W. Ren, T. Wang, C. Li, and X. Cao, "Under-Display Camera Image Enhancement via Cascaded Curve Estimation," *IEEE Transactions on Image Processing*, vol. 31, pp. 4856–4868, 2022.
- [6] Y. Zhou, Y. Song, and X. Du, "Modular Degradation Simulation and Restoration for Under-Display Camera," Sep. 2022.
- [7] B. Song, X. Chen, S. Xu, and J. Zhou, "Under-Display Camera Image Restoration with Scattering Effect," Aug. 2023.
- [8] J. Tan, X. Chen, T. Wang, K. Zhang, W. Luo, and X. Cao, "Blind face restoration for under-display camera via dictionary guided transformer," *IEEE Transactions on Circuits and Systems for Video Technology*, 2023.
- [9] X. Chen, T. Wang, Z. Shao, K. Zhang, W. Luo, T. Lu, Z. Liu, T.-K. Kim, and H. Li, "Deep video restoration for under-display camera," *arXiv preprint arXiv:2309.04752*, 2023.
- [10] Z. Wang, K. Zhang, and R. Sankaranarayanan, "Lrdif: Diffusion models for under-display camera emotion recognition," *arXiv preprint arXiv:2402.00250*, 2024.
- [11] K. Rossmann, "Point spread-function, line spread-function, and modulation transfer function: tools for the study of imaging systems," *Radiology*, vol. 93, no. 2, pp. 257–272, 1969.
- [12] K. Fukushima, S. Miyake, and T. Ito, "Neocognitron: A neural network model for a mechanism of visual pattern recognition," *IEEE transactions on systems, man, and cybernetics*, no. 5, pp. 826–834, 1983.
- [13] S. Li, S. Xu, W. Ma, and Q. Zong, "Image manipulation localization using attentional cross-domain cnn features," *IEEE Transactions on Neural Networks and Learning Systems*, vol. 34, no. 9, pp. 5614–5628, 2023.
- [14] Y. Chen, X. Dai, M. Liu, D. Chen, L. Yuan, and Z. Liu, "Dynamic convolution: Attention over convolution kernels," in *Proceedings of the IEEE/CVF conference on computer vision and pattern recognition*, 2020, pp. 11 030–11 039.
- [15] A. Vaswani, N. Shazeer, N. Parmar, J. Uszkoreit, L. Jones, A. N. Gomez, \. Kaiser, and I. Polosukhin, "Attention is all you need," *Advances in neural information processing systems*, vol. 30, 2017.
- [16] A. Dosovitskiy, L. Beyer, A. Kolesnikov, D. Weissenborn, X. Zhai, T. Unterthiner, M. Dehghani, M. Minderer, G. Heigold, and S. Gelly, "An image is worth 16x16 words: Transformers for image recognition at scale," *arXiv preprint arXiv:2010.11929*, 2020.
- [17] K. Zhang, W. Ren, W. Luo, W.-S. Lai, B. Stenger, M.-H. Yang, and H. Li, "Deep image deblurring: A survey," *International Journal of Computer Vision*, vol. 130, no. 9, pp. 2103–2130, 2022.
- [18] Z. Zhang, Z. Song, K. Zhang, W. Luo, Z. Fan, and J. Lu, "Benchmarking ultra-high-definition image reflection removal," *arXiv preprint arXiv:2308.00265*, 2023.
- [19] S. Alfasly, C. K. Chui, Q. Jiang, J. Lu, and C. Xu, "An effective video transformer with synchronized spatiotemporal and spatial self-attention for action recognition," *IEEE Transactions on Neural Networks and Learning Systems*, vol. 35, no. 2, pp. 2496–2509, 2024.
- [20] A. Madry, A. Makelov, L. Schmidt, D. Tsipras, and A. Vladu, "Towards deep learning models resistant to adversarial attacks," in *ICLR*, 2018. [Online]. Available: <https://openreview.net/forum?id=rJzIBfZab>
- [21] N. Carlini and D. Wagner, "Towards Evaluating the Robustness of Neural Networks," Mar. 2017.
- [22] C. Guo, J. R. Gardner, Y. You, A. G. Wilson, and K. Q. Weinberger, "Simple Black-box Adversarial Attacks," Aug. 2019.
- [23] M. Andriushchenko, F. Croce, N. Flammarion, and M. Hein, "Square Attack: A query-efficient black-box adversarial attack via random search," Jul. 2020.
- [24] J. Ho, A. Jain, and P. Abbeel, "Denoising Diffusion Probabilistic Models," Dec. 2020.
- [25] A. Vahdat, K. Kreis, and J. Kautz, "Score-based Generative Modeling in Latent Space," Dec. 2021.
- [26] W. Nie, B. Guo, Y. Huang, C. Xiao, A. Vahdat, and A. Anandkumar, "Diffusion Models for Adversarial Purification," May 2022.
- [27] Y. Zhou, M. Kwan, K. Tolentino, N. Emerton, S. Lim, T. Large, L. Fu, Z. Pan, B. Li, Q. Yang, Y. Liu, J. Tang, T. Ku, S. Ma, B. Hu, J. Wang, D. Puthussery, H. P. S. M. Kuriakose, J. C. V. V. Sundar, S. Hegde, D. Kothandaraman, K. Mitra, A. Jassal, N. A. Shah, S. Nathan, N. A. E. Rahel, D. Chen, S. Nie, S. Yin, C. Ma, H. Wang, T. Zhao, S. Zhao, J. Rego, H. Chen, S. Li, Z. Hu, K. W. Lau, L.-M. Po, D. Yu, Y. A. U. Rehman, Y. Li, and L. Xing, "UDC 2020 Challenge on Image Restoration of Under-Display Camera: Methods and Results," Aug. 2020.
- [28] O. Ronneberger, P. Fischer, and T. Brox, "U-Net: Convolutional Networks for Biomedical Image Segmentation," May 2015.
- [29] V. Sundar, S. Hegde, D. Kothandaraman, and K. Mitra, "Deep Atrous Guided Filter for Image Restoration in Under Display Cameras," Sep. 2020.
- [30] P. Isola, J.-Y. Zhu, T. Zhou, and A. A. Efros, "Image-to-image translation with conditional adversarial networks," in *Proceedings of the IEEE Conference on Computer Vision and Pattern Recognition*, 2017, pp. 1125–1134.
- [31] C. Szegedy, W. Zaremba, I. Sutskever, J. Bruna, D. Erhan, I. Goodfellow, and R. Fergus, "Intriguing properties of neural networks," Feb. 2014.
- [32] H. Xu, Y. Ma, H.-C. Liu, D. Deb, H. Liu, J.-L. Tang, and A. K. Jain, "Adversarial attacks and defenses in images, graphs and text: A review," *International Journal of Automation and Computing*, vol. 17, no. 2, pp. 151–178, 2020.
- [33] C. Szegedy, W. Zaremba, I. Sutskever, J. Bruna, D. Erhan, I. J. Goodfellow, and R. Fergus, "Intriguing properties of neural networks," in *ICLR*, 2014.
- [34] I. J. Goodfellow, J. Shlens, and C. Szegedy, "Explaining and harnessing adversarial examples," in *ICLR*, 2015. [Online]. Available: <http://arxiv.org/abs/1412.6572>
- [35] S.-M. Moosavi-Dezfooli, A. Fawzi, and P. Frossard, "Deepfool: A simple and accurate method to fool deep neural networks," in *CVPR*, 2016, pp. 2574–2582.
- [36] P.-Y. Chen, H. Zhang, Y. Sharma, J. Yi, and C.-J. Hsieh, "ZOO: Zeroth Order Optimization based Black-box Attacks to Deep Neural Networks without Training Substitute Models," Nov. 2017.
- [37] A. Rahmati, S.-M. Moosavi-Dezfooli, P. Frossard, and H. Dai, "GeoDA: A geometric framework for black-box adversarial attacks," Mar. 2020.
- [38] K. V. Gandikota, P. Chandramouli, and M. Moeller, "On Adversarial Robustness of Deep Image Deblurring," in *2022 IEEE International Conference on Image Processing (ICIP)*. IEEE, 2022, pp. 3161–3165.
- [39] Y. Yu, W. Yang, Y.-P. Tan, and A. C. Kot, "Towards Robust Rain Removal Against Adversarial Attacks: A Comprehensive Benchmark Analysis and Beyond," in *Proceedings of the IEEE/CVF Conference on Computer Vision and Pattern Recognition*, 2022, pp. 6013–6022.
- [40] J. Gui, X. Cong, C. Peng, Y. Y. Tang, and J. T.-Y. Kwok, "Adversarial Attack and Defense for Dehazing Networks," *arXiv preprint arXiv:2303.17255*, 2023.
- [41] J. X. Morris, E. Lifland, J. Y. Yoo, J. Grigsby, D. Jin, and Y. Qi, "TextAttack: A Framework for Adversarial Attacks, Data Augmentation, and Adversarial Training in NLP," Oct. 2020.
- [42] H. Zhuang, Y. Zhang, and S. Liu, "A Pilot Study of Query-Free Adversarial Attack against Stable Diffusion," in *2023 IEEE/CVF Conference on Computer Vision and Pattern Recognition Workshops (CVPRW)*. Vancouver, BC, Canada: IEEE, Jun. 2023, pp. 2385–2392.
- [43] I. J. Goodfellow, J. Shlens, and C. Szegedy, "Explaining and harnessing adversarial examples," *arXiv preprint arXiv:1412.6572*, 2014.
- [44] A. Madry, A. Makelov, L. Schmidt, D. Tsipras, and A. Vladu, "Towards deep learning models resistant to adversarial attacks," *arXiv preprint arXiv:1706.06083*, 2017.
- [45] L. Schott, J. Rauber, M. Bethge, and W. Brendel, "Towards the first adversarially robust neural network model on mnist," *arXiv preprint arXiv:1805.09190*, 2018.
- [46] G. W. Ding, K. Y. C. Lui, X. Jin, L. Wang, and R. Huang, "On the sensitivity of adversarial robustness to input data distributions." *ICLR (Poster)*, vol. 4, 2019.
- [47] C. Guo, M. Rana, M. Cisse, and L. Van Der Maaten, "Countering adversarial images using input transformations," *arXiv preprint arXiv:1711.00117*, 2017.
- [48] X. Jia, X. Wei, X. Cao, and H. Foroosh, "Comdefend: An efficient image compression model to defend adversarial examples," in *Proceedings of the IEEE/CVF conference on computer vision and pattern recognition*, 2019, pp. 6084–6092.
- [49] D. P. Kingma and M. Welling, "Auto-Encoding Variational Bayes," Dec. 2022.

- [50] P. Samangouei, M. Kabkab, and R. Chellappa, "Defense-GAN: Protecting Classifiers Against Adversarial Attacks Using Generative Models," May 2018.
- [51] J. Zhou, C. Liang, and J. Chen, "Manifold Projection for Adversarial Defense on Face Recognition," in *Computer Vision – ECCV 2020*, A. Vedaldi, H. Bischof, T. Brox, and J.-M. Frahm, Eds. Cham: Springer International Publishing, 2020, vol. 12375, pp. 288–305.
- [52] Y. Yu, W. Yang, Y.-P. Tan, and A. C. Kot, "Towards robust rain removal against adversarial attacks: A comprehensive benchmark analysis and beyond," in *Proceedings of the IEEE/CVF Conference on Computer Vision and Pattern Recognition*, 2022, pp. 6013–6022.
- [53] A. Mustafa, S. H. Khan, M. Hayat, J. Shen, and L. Shao, "Image super-resolution as a defense against adversarial attacks," *IEEE Transactions on Image Processing*, vol. 29, pp. 1711–1724, 2019.
- [54] J.-H. Choi, H. Zhang, J.-H. Kim, C.-J. Hsieh, and J.-S. Lee, "Evaluating robustness of deep image super-resolution against adversarial attacks," in *Proceedings of the IEEE/CVF International Conference on Computer Vision*, 2019, pp. 303–311.
- [55] J. Yue, H. Li, P. Wei, G. Li, and L. Lin, "Robust real-world image super-resolution against adversarial attacks," in *Proceedings of the 29th ACM International Conference on Multimedia*, 2021, pp. 5148–5157.
- [56] Z. Song, Z. Zhang, K. Zhang, W. Luo, Z. Fan, W. Ren, and J. Lu, "Robust Single Image Reflection Removal Against Adversarial Attacks," in *Proceedings of the IEEE/CVF Conference on Computer Vision and Pattern Recognition*, 2023.
- [57] R. Zhang, P. Isola, A. A. Efros, E. Shechtman, and O. Wang, "The unreasonable effectiveness of deep features as a perceptual metric," in *CVPR*, 2018, pp. 586–595.
- [58] Z. Wang, X. Cun, J. Bao, W. Zhou, J. Liu, and H. Li, "Uformer: A General U-Shaped Transformer for Image Restoration," in *2022 IEEE/CVF Conference on Computer Vision and Pattern Recognition (CVPR)*. New Orleans, LA, USA: IEEE, Jun. 2022, pp. 17 662–17 672.
- [59] Z. Dong, P. Wei, and L. Lin, "Adversarially-Aware Robust Object Detector," Jul. 2022.
- [60] Z. Wang, Z. Zhang, X. Zhang, H. Zheng, M. Zhou, Y. Zhang, and Y. Wang, "DR2: Diffusion-Based Robust Degradation Remover for Blind Face Restoration," in *2023 IEEE/CVF Conference on Computer Vision and Pattern Recognition (CVPR)*. Vancouver, BC, Canada: IEEE, Jun. 2023, pp. 1704–1713.
- [61] A. Yang and A. C. Sankaranarayanan, "Designing display pixel layouts for under-panel cameras," *IEEE Transactions on Pattern Analysis and Machine Intelligence*, vol. 43, no. 7, pp. 2245–2256, 2021.
- [62] "HDRIs • Poly Haven," <https://polyhaven.com/hdris>.
- [63] Z. Wang, A. C. Bovik, H. R. Sheikh, and E. P. Simoncelli, "Image quality assessment: from error visibility to structural similarity," *IEEE transactions on image processing*, vol. 13, no. 4, pp. 600–612, 2004.
- [64] R. Zhang, P. Isola, A. A. Efros, E. Shechtman, and O. Wang, "The unreasonable effectiveness of deep features as a perceptual metric," in *Proceedings of the IEEE conference on computer vision and pattern recognition*, 2018, pp. 586–595.
- [65] K. Simonyan and A. Zisserman, "Very deep convolutional networks for large-scale image recognition," *arXiv preprint arXiv:1409.1556*, 2014.